Electronic Supplementary Material (ESI) for Journal of Materials Chemistry C.
This journal is © The Royal Society of Chemistry 2020

Supporting Information

Unconventional out-of-plane domain inversion via in-plane ionic migration in a van der Waals ferroelectric

*Dong-Dong Xu[a‡], Ru-Ru Ma[a‡], Yi-Feng Zhao[a], Zhao Guan[a], Qi-Lan Zhong[a], Rong Huang[a], Ping-Hua Xiang[*a, b], Ni Zhong[*a, b], and Chun-Gang Duan[a,b]*

a. Key Laboratory of Polar Materials and Devices (MOE) and Department of Electronics, East China Normal University, Shanghai, 200241, China

b. Collaborative Innovation Center of Extreme Optics, Shanxi University, Taiyuan, Shanxi 030006, China

* E-mail: nzhong@ee.ecnu.edu.cn

* E-mail: phxiang@ee.ecnu.edu.cn

EXPERIMENTAL SECTION

PFM measurements: Our devices were fabricated by traditional lithography techniques. Single crystal $CuInP_2S_6$ samples were purchased from HQ Graphene. PFM measurements were performed on a commercial atomic force microscope (Asylum Cypher). Conductive Pt-coated silicon cantilevers (NSC 18, Mikromasch) were used for all imaging mode. A soft tip with a spring constant of 2.8 $N \cdot m^{-1}$ and a typical free resonance of 75 kHz was driven with an ac voltage (V_{ac} = 0.8-1.0 V) under the tip-sample contact resonant frequency. Typically, a contact mode set point of 0.2 V was used. PFM imaging was performed at a single frequency close to the contact resonance frequency (~300 kHz) with the help of a function generator and an external lock-in.

Raman spectroscopy measurements: Raman spectrum was conducted on a Renishaw inVia Raman microscope equipped with a liquid-nitrogen-cooled CCD and a ×100 objective lens (NA = 0.85). The excitation wavelength is 532 nm with a spatial resolution of 0.76 µm.

SEM and EDS measurements: The surface morphologies were characterized by field-emission scanning electron microscope (FIB, Helios G4 UX, FEI Inc. USA)， which equipped with an X-ray energy dispersive spectrometer (EDS: X-Max 150T, Oxford, UK) for chemical composition analyses.

First-principles calculations: First-principles calculations were carried out with the Vienna ab initio Simulation Package (VASP)[1] by using the projector-augmented wave (PAW) method[2] and the generalized gradient approximation(GGA).The exchange-correlation potential is adopted in the PBE (Perdew-Burke-Ernzerh) method.[3] Both structural relaxation and self-consistent calculations were carried out with the tetrahedral method with Blöchl corrections,[4] and the energy cut-off is set to 500eV. We fully optimize each ionic position until the residual forces

converged less than 0.001 eV/Å and self-consistent convergence for electronic energy is 10^{-6} eV. A 12×12×1 Monkhorst-Pack *k*-point mesh is adopted for the geometry optimization. A vacuum space of 20 Å is used to avoid interactions between periodically repeated layers.

References:

1. G. Kresse, J. Furthmuller, *Comp. Mater. Sci.* **1996**, *6*, 15.
2. P. E. Blöchl, *Phys. Rev. B* **1994**, *50*, 17953.
3. J. P. Perdew, K. Burke, M. Ernzerhof, *Phys. Rev. Lett.* **1996**, *77*, 3865.
4. P. E. Blöchl, O. Jepsen, O. K. Andersen, *Phys. Rev. B* **1994**, *49*, 16223.

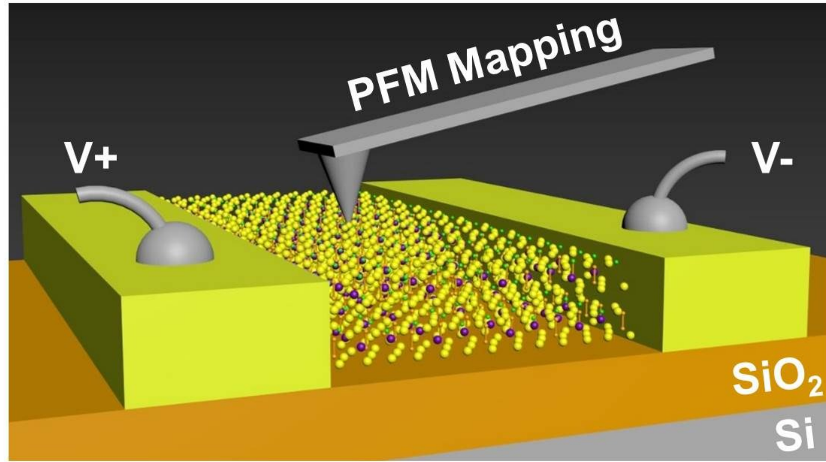

Fig. S1 The schematic diagram of test configuration consisted of a PFM system and a planar device.

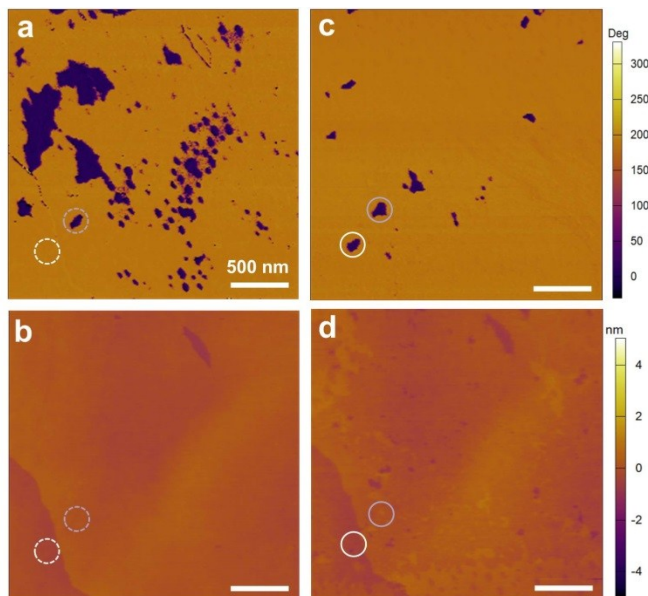

Fig. S2 (a-b) The PFM phase (a) and the corresponding AFM topography (b) for 240-nm-thick flakes. (c-d) The PFM phase (c) and the corresponding AFM topography (d) for biased 240-nm-thick flakes.

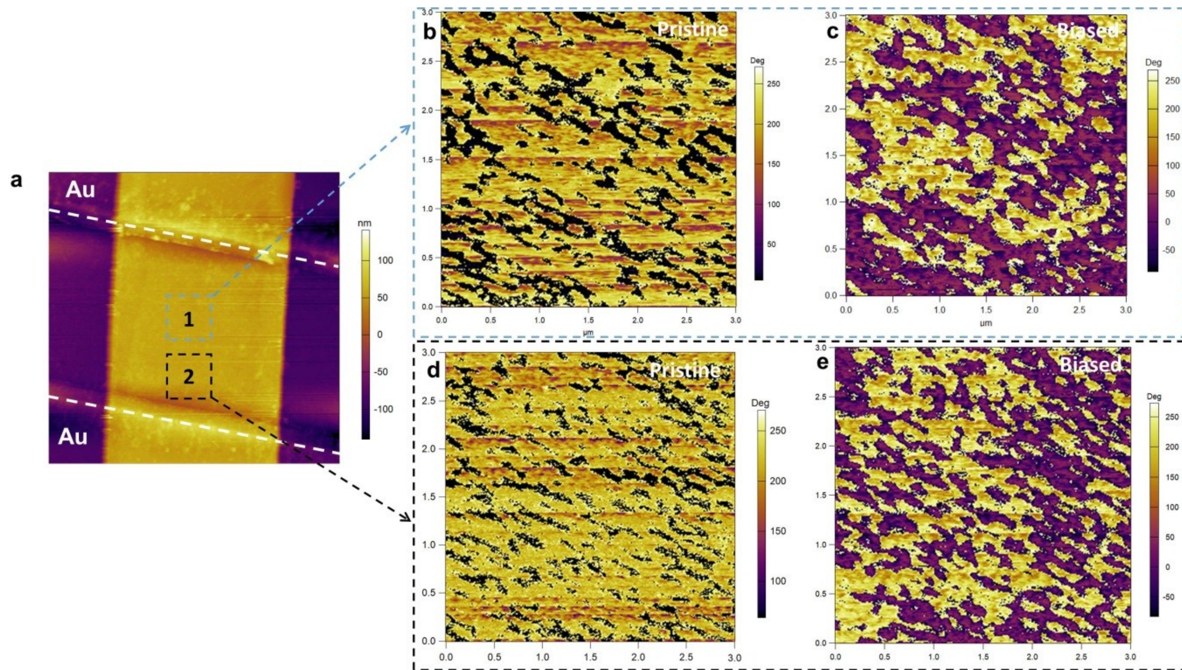

Fig. S3. Domain inversion induced by an in-plane electric filed. (a) AFM morphology of a two-terminal device equipped with Au electrodes. (b, d) The pristine phase states of regions 1 and 2, respectively, in an 80-nm-thick CIPS flake. (d, e) The changed phase states after the application of a 4 V bias.

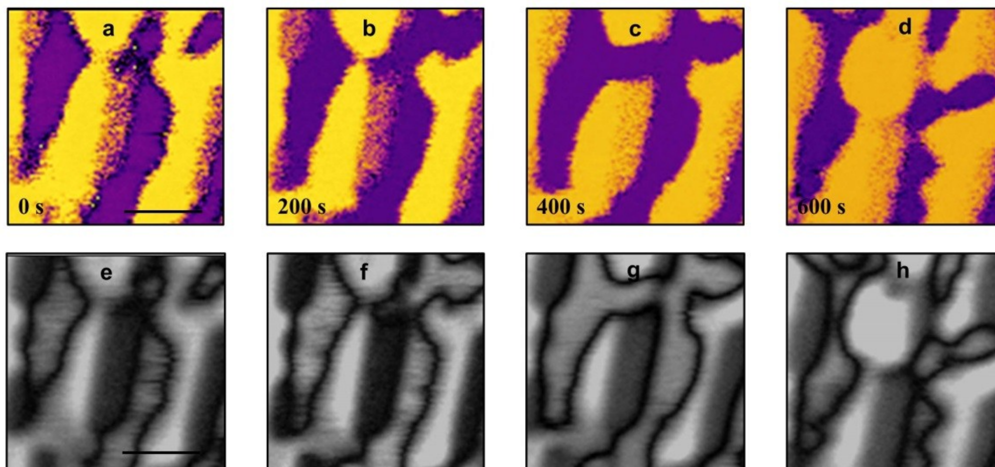

Fig. S4. A time evolution of phase (up panel) and corresponding amplitude signals (down panel) after the application of a 4 V voltage.

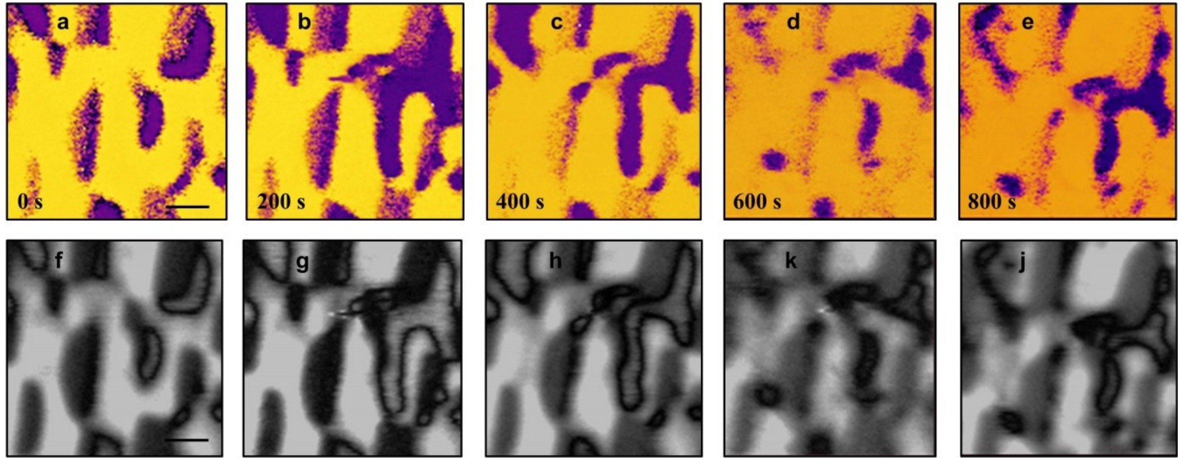

Fig. S5. Anther experimental case for the evolution of phase (up panel) and corresponding amplitude signals (down panel) after the application of a 4 V voltage.

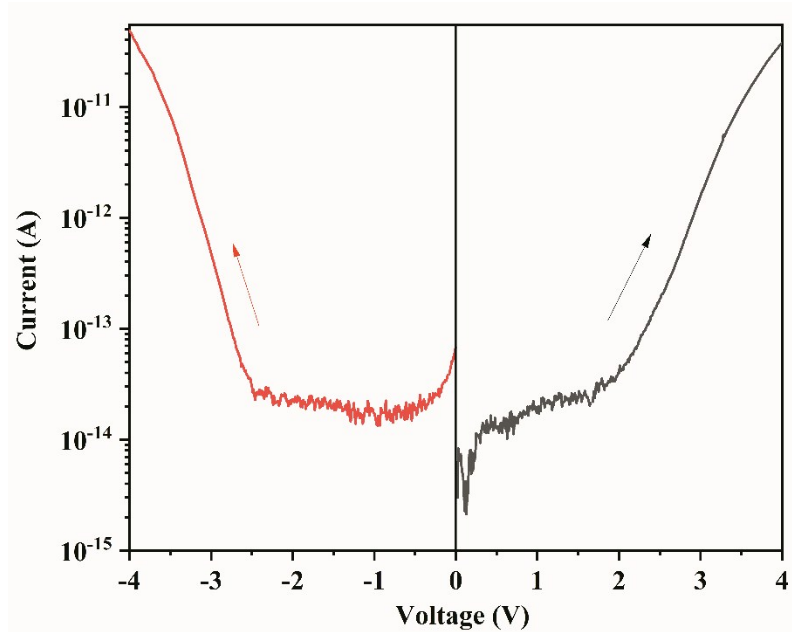

Fig. S6. Current-voltage curves along opposite scan directions.

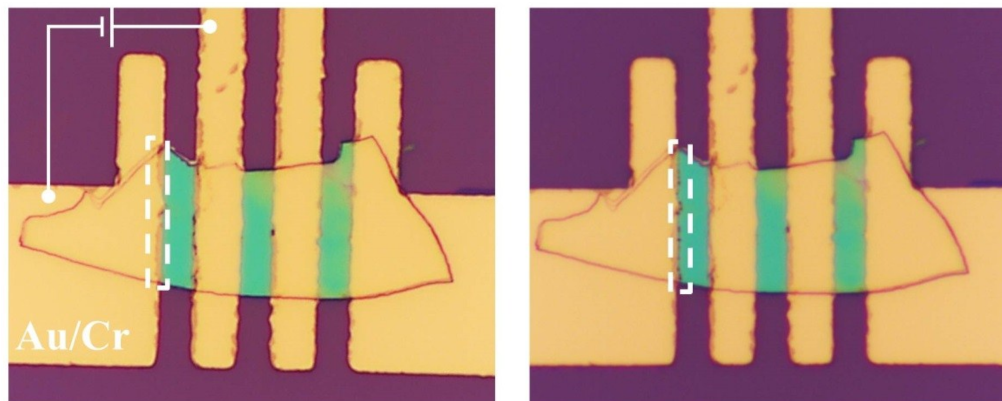

Fig. S7. The comparison of device pictures before (a) and after (b) the application of 4 V at 373 K. Some dispersed nanoparticles were observed.

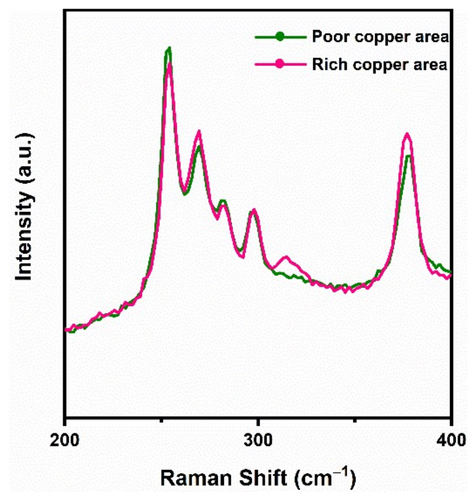

Fig. S8. The corresponding Raman spectra of poor/rich copper areas.

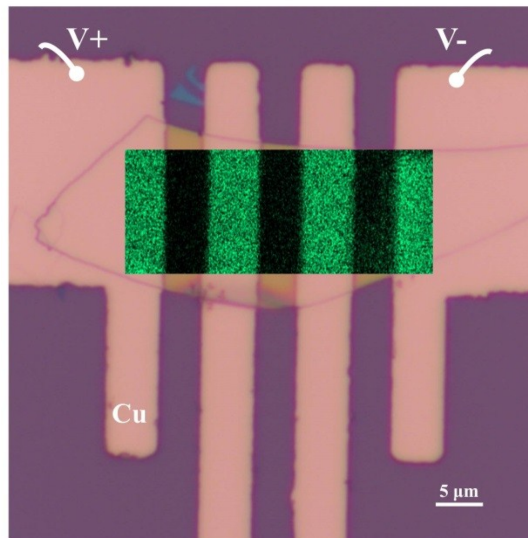

Fig. S9 A device picture with Cu electrodes. The inset is Cu element mapping which exhibits graded distribution along the direction of the electric field.

Table S1. The selected possible crystallographic sites that Cu ions may pass through during the migration process.

Atoms	***X/a***	***y/b***	***z/c***
Cu1	0.166	0.667	0.554
Cu2	0.666	0.666	0.550
Cu3	0.600	0.660	0.524
Cu4	0.270	0.660	0.470
Cu5	0.23	0.660	0.480
Cu6	0.600	0.660	0.460
Cu7	0.660	0.660	0.445
Cu8	0.400	0.660	0.500
Cu9	0.220	0.660	0.500
Cu10	0.524	0.660	0.524